Growth, Morphology, and Structure of Boron Nitride Nanotubes

Renzhi Ma,* Yoshio Bando,* Tadao Sato, and Keiji Kurashima

National Institute for Materials Science·Advanced Materials Laboratory, Tsukuba, Ibaraki 305-0044, Japan

Received March 29, 2001. Revised Manuscript Received June 18, 2001

Multiwalled BN nanotubes were synthesized via a chemical vapor deposition (CVD) route from a $B_4N_3O_2H$ precursor. Their morphological and structural features have been studied. It was suggested that the tips encapsulate boron oxynitride nanoclusters, which incorporate silicon, aluminum, and calcium and serve as the effective promoters for CVD growth of the BN nanotubes. An alternative open-end growth mechanism is also applied for the occasional formation of nanotubes with open or flat tip ends. Local three-dimensional ordering in the nanotube shell assembly was often observed. BN nanotubes synthesized in the current CVD process exhibit a dominant near zigzag arrangement and a rhombohedral (r-BN) stacking order. The results of initial efforts to grow arrays of aligned BN nanotubes are also described.

Introduction

Boron nitride nanotubes (BN-NTs) have been of considerable research interest in recent years.[1−9] Besides their excellent chemical stability and heat resistance, BN nanotubes are predicted to be wide gap semiconductors having an electronic band gap independent of diameter and chirality.[1] The earlier work of Hamilton et al. showed the formation of a tubular structure for BN from 2,4,6-trichloroborazine and alkali metals.[2,3] Recently, various production methods for BN nanotubes and the associated growth mechanisms have been developed.[4−9] Metal clusters (W-, Hf-, Ta-, Zr-based) originating from electrodes were often observed near the tip ends in the arc-discharge synthesis.[4−7] Mo clusters were also found to be encapsulated at the tip ends of the BN tubes in the MoO_3-promoted synthesis from carbon nanotube templates.[9] It has been suggested that these metal encapsulates may play a catalytic or promoting role during BN tube growth.

Unlike C nanotubes routinely synthesized from metal-catalyzed (Fe-, Co-, Ni-based) chemical vapor deposition (CVD) processes,[10,11] previous CVD efforts yielded BN nanotubes having segmented (bamboo-like) structures[12−14] or poorly crystalline walls.[12] Recently, the CVD growth of hollow, crystalline BN nanotubes on nickel boride particles by pyrolysis of $B_3N_3H_6$ has been reported.[15] The nickel boride particles used there are in the micrometer range, which is far beyond the usual nanometer dimension of the catalyst particles employed in the CVD method. In addition, CVD is widely used to grow self-assembled or aligned carbon nanotubes (CNTs) on various substrates.[16−19] Such a kind of substrate−C-NT system may have great potential application for electronic devices, e.g., panel displays based on field emission. Similarly, it would be of interest to grow aligned BN-NTs on certain substrates. To our knowledge, there has been only one prior study where aligned arrays of BN nanotubes were successfully fabricated within the pores of anodic aluminum oxide.[20]

There have been some experimental observations that BN nanotubes are commonly observed having flat tip

* Corresponding authors. Fax: +81-298-51-6280. E-mail addresses: Ma.Renzhi@nims.go.jp and BANDO.Yoshio@nims.go.jp.

(1) Blase, X.; Rubio, A.; Louie, S. G.; Cohen, M. L. *Europhys. Lett.* **1994**, *28*, 335.
(2) Hamilton, E. J. M.; Dolan, S. E.; Mann C. E.; Colijin, H. O.; McDonald, C. A.; Shore, S. G. *Science* **1993**, *260*, 659.
(3) Hamilton, E. J. M.; Dolan, S. E.; Mann C. E.; Colijin, H. O.; Shore, S. G. *Chem, Mater.* **1995**, *7*, 111.
(4) Chopra, N. G.; Luyken, R. J.; Cherrey, K.; Crespi, V. H.; Cohen, M. L.; Louie, S. G.; Zettle, A. *Science* **1995**, *69*, 966.
(5) Loiseau, A.; Willaime, F.; Demoncy, N.; Hug, G.; Pascard, H. *Phys. Rev. Lett.* **1996**, *76*, 4737.
(6) Terrones, M.; Hsu, W. K.; Terrones, H.; Zhang, J. P.; Ramos, S.; Hare, J. P.; Castillo, R.; Prassides, K.; Cheetham, A. K.; Kroto, H. W.; Walton, D. R. M. *Chem. Phys. Lett.* **1996**, *259*, 568.
(7) Saito, Y., Maida, M.; Mastumoto, T. *Jpn. J. Appl. Phys.* **1999**, *38*, 159.
(8) Han, W.; Bando, Y.; Kurashima, K.; Sato, T. *Appl. Phys. Lett.* **1998**, *73*, 3085.
(9) Golberg, D.; Bando, Y.; Kurashima, K.; Sato, T. *Chem. Phys. Lett.* **2000**, *323*, 185.
(10) Ivanov, V.; Nagy, J. B.; Lambin, Ph.; Lucas, A.; Zhang, X. B.; Zhang, X. F.; Bernaerts, D.; Tendeloo, G. Van; Amelinckx, S.; Landuyt, J. Van. *Chem. Phys. Lett.* **1994**, *223*, 329.
(11) Dai, H.; Rinzler, A. G.; Nikolaev, P.; Thess, A.; Colbert, D. T.; Smalley, R. E. *Chem. Phys. Lett.* **1996**, *260*, 471.
(12) Gleize, P.; Schouler, M. C.; Gadelle, P.; Caillet, M. *J. Mater. Sci.* **1994**, *29*, 1575.
(13) Sen, R.; Satishkumar, B. C.; Govindaraj, A.; Harikumar, K. R.; Raina, G.; Zhang, J. P.; Cheetham, A. K.; Rao, C. N. R. *Chem. Phys. Lett.* **1998**, *287*, 671.
(14) Bourgeois, L.; Bando, Y.; Sato, T. *J. Phys. D: Appl. Phys.* **2000**, *33*, 1902.
(15) Lourie, O. R.; Jones, C. R.; Bartlett, B. M.; Gibbons, P. C.; Ruoff, R. S.; Buhro, W. E. *Chem. Mater.* **2000**, *12*, 1808.
(16) Li, W. Z.; Xie, S. S.; Qian, L. X.; Chang, B. H.; Zou, B. S.; Zhou, W. Y.; Zhao, A.; Wang, G. *Science* **1996**, *274*, 1701.
(17) Terrones, M.; Grobert, N.; Olivares, J.; Zhang, J. P.; Terrones, H.; Kordatos, K.; Hsu, W. K.; Hare, J. P.; Townsend, P. D.; Prassides, K.; Cheetham, A. K.; Kroto, H. W.; Walton, D. R. M. *Nature* **1997**, *388*, 52.
(18) Ren, Z. F.; Huang, Z. P.; Xu, J. W.; Wang, J. H.; Bush, P.; Siegal, M. P.; Provencio, P. N. *Science* **1998**, *282*, 1105.
(19) Fan, S. S.; Chapline, M. G.; Franklin, N. R.; Tombler, T. W.; Cassell, A. M.;. Dai, H. J. *Science* **1999**, *283*, 512.
(20) Shelimov, K. B.; Moskovits, M. *Chem. Mater.* **2000**, *12*, 250.

10.1021/cm0102741 CCC: $20.00
Published on Web 08/24/2001

caps.[5,6,21] Furthermore, some authors have determined the preponderance of the zigzag arrangement in BN nanotubes produced by laser heating at high pressure,[22] by substitution from carbon nanotube templates,[9,21] or by thermal annealing of a mixed powder of β-rhombohedral boron and hexagonal BN at 1200 °C under lithium vapor.[23] Contrary to the usually turbostratic stacking in C nanotubes, near three-dimensional ordering is observed in bamboo-like BN nanotubes[14] and in BN nanotubes synthesized from carbon nanotube templates.[24] Concerning the CVD-grown BN nanotubes, there is still much that is not known about the structural features.

We have previously reported a specifically designed CVD route to BN nanotubes from a $B_4N_3O_2H$ precursor, where the nanoclusters encapsulated in the bulbous tips of the tubes were considered to be playing the catalytic role.[25] In the current work, we present an in-depth morphological and structural analysis of the BN nanotubes synthesized from the $B_4N_3O_2H$ precursor. It may bring us closer to a better understanding of the CVD growth of BN nanotubes. In addition, preliminary results on the growth of nearly aligned BN nanotubes are also presented.

Experimental Section

The BN nanotubes were synthesized from a CVD method employing a B−N−O precursor.[25] The precursor was prepared in a reaction essentially similar to that described in ref 26. First, 0.4 mol of boric acid (H_3BO_3, Junsei Chemical Co. Ltd.) was dissolved in 1000 mL of water at 100 °C. Then 0.2 mol of melamine ($C_3N_6H_6$, Wako Pure Chemical Industrial Ltd.) was added slowly into the solution. White powders began to precipitate by cooling the hot solution to room temperature. The solution was kept under room temperature for 2 days to fulfill the precipitating process. The precipitated white powder was calcined at 500 °C in air for 3 h. After an additional 1 h of annealing at 800 °C in N_2, the finally obtained powder might be $B_4N_3O_2H$ based on the following chemical reaction: $2(C_3N_6H_6{\cdot}2H_3BO_3) \rightarrow B_4N_3O_2H + 4H_2NCN + 2CO_2 + NH_3 + 6H_2O$.[26]

The precursor was charged into a graphite crucible, itself placed into a graphite susceptor. A RF induction furnace was used for heating the susceptor to 1700 °C. The susceptor was held in a flowing N_2 atmosphere (1l/min.) at 1700 °C for 2 h. The N_2 stream, bubbling from distilled water, was arranged to pass through carbon black or polyacrylonitrile (PAN)-based carbon fibers at 1500 °C before it was introduced into the susceptor. Boric oxide vapor, generated from the precursor upon decomposition, was reduced into BN nanotubes according to $B_2O_3 + 4C + H_2O + N_2 \rightarrow 2BN + 4CO + H_2$.[25] BN nanotubes were deposited as whitish powders on the walls of the graphite crucible, where the temperature is on the order of 1200 °C. The yield of the BN nanotubes depends on the amount of precursor used. Usually 3 mg of raw products can be obtained from 2 g of $B_4N_3O_2H$. In some experimental runs, some PAN-based carbon fibers were placed in the 1200 °C temperature region to serve as the substrate for BN nanotube deposition.

Figure 1. SEM images of the CVD-grown BN nanotubes from $B_4N_3O_2H$ precursor.

The raw materials removed from the walls were observed by scanning electron microscopy (SEM). Sample powders were also ultrasonically dispersed in CCl_4 and dropped onto a carbon-coated-copper grid. The characterization was carried out by using a JEM-3000F (JEOL) high-resolution transmission field emission electron microscope (HRTEM) operated at 300 kV. Energy-dispersive X-ray analysis (EDX) and electron energy loss spectroscopy (EELS) were employed in identifying the elemental composition of the tubes and tip encapsulates.

Results and Discussions

SEM examination of the raw white deposits reveals an abundance of BN nanotubes (Figure 1). Most of the tube tips appear to have higher atomic densities than the tube body as they exhibit brighter contrast under SEM observation. As shown in Figure 2, TEM images established that they are hollow, multiwalled nanotubes, exhibiting different tip morphologies. In addition to bulbous tips as described in the previous report[25] (Figure 2a), pear-shaped darker inclusions wedged in the tip ends (Figure 2b) are also observed. We found that the bulbous tips are dominant when the N_2 gas stream was arranged to pass through carbon black. On the other hand, pear-shaped tip inclusions are often observed if the carbon black was changed into PAN-based carbon fibers. From the atomic emission (AE) spectra generated by an arc source, the PAN-based fibers were detected to contain Si as the main impurity and a little Ca, while the carbon black had a high purity except for a little B (Table 1). So it is reasonable to consider that the different impurity levels led to different tip morphologies.

EDX and EELS measurements showed that most of the tip inclusions, either bulbous or pear-shaped, consist mainly of B, N, and O. The difference is that the pear-shaped ones were found to contain more impurities, such as Si, Al, and Ca. A typical EDX spectrum from the tip inclusions (arrow in Figure 2b) is shown in Figure 3a. For comparison, the EDX spectrum taken from the tube body is also shown (Figure 3b). In the spectra, the Cu peaks and low-intensity Ti peak originate from the Cu mesh of the TEM grid and from the TEM holder. As the tip inclusions are surrounded with BN layers, the outer BN layers may also contribute to

(21) Golberg, D.; Han, W.; Bando, Y.; Bourgeois, L.; Kurashima, K.; Sato, T. *J. Appl. Phys.* **1999**, *86*, 2364.
(22) Golberg, D.; Bando, Y.; Eremets, M.; Takemura, K.; Kurashima, K.; Yusa, H. *Appl. Phys. Lett.* **1996**, *69*, 2045.
(23) Terauchi, M.; Tanaka, M.; Suzuki, K.; Ogino, A.; Kimura, K. *Chem. phys. Lett.* **2000**, *324*, 359.
(24) Golberg, D.; Bando, Y.; Bourgeois, L.; Kurashima, K.; Sato, T. *Appl. Phys. Lett.* **2000**, *77*, 1979.
(25) Ma, R.; Bando, Y.; Sato, T. *Chem. Phys. Lett.* **2001**, *337*, 61.
(26) Hagio, T.; Kobayashi K.; Sato T. *J. Ceram. Soc. Jpn.* **1994**, *102*, 1051.

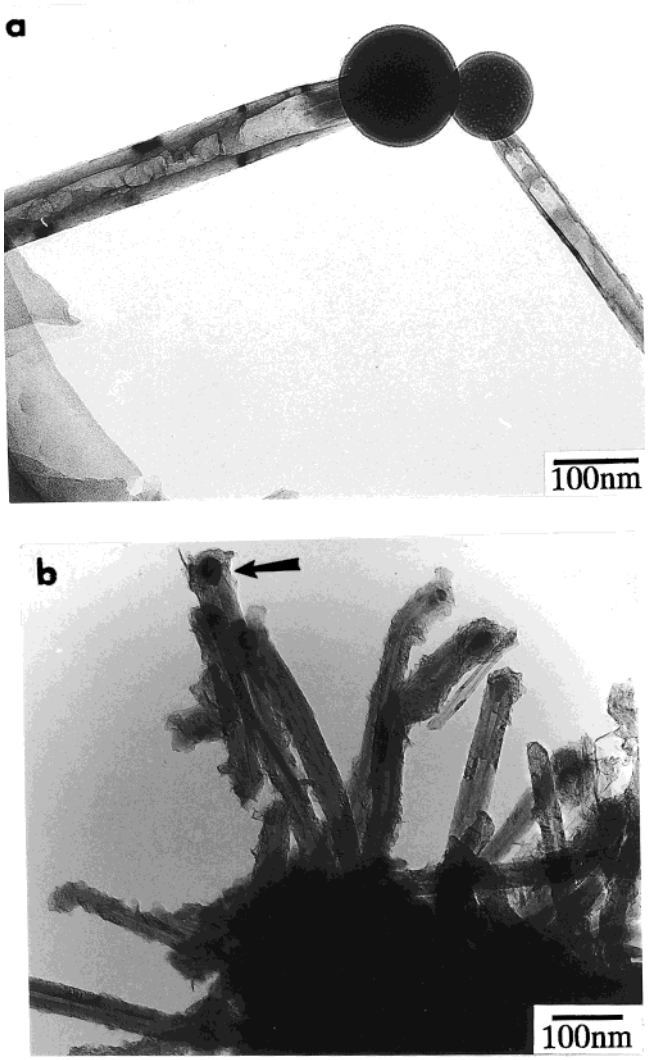

Figure 2. Low-magnification TEM images of BN nanotubes with different tip morphologies: (a) bulbous tips and (b) the darker contrast encapsulates wedged in the tube tip ends.

Table 1. Impurities in Carbon Black and PAN-Based Carbon Fiber

impurities (wt %)	B	Si	Ca	Na	K
carbon black	0.030	a	a	a	a
carbon fiber	a	0.10	0.030	0.010	0.010

[a] Below detect limitation.

the B and N scattering intensities in Figure 3a. This kind of overlapping makes it rather difficult to identify the exact composition of the inclusions. In fact, it was found that the relative contents of Si, Al, and Ca in the inclusions are not fixed but vary from tip to tip. From the rough analysis of the recorded spectra, it is more reasonable to suggest that the inclusions are some B−N−O nanoclusters, with incorporation of Si, Al, and Ca, rather than stoichiometric compounds. The sources of Si, Al, and Ca are considered to be derived from the impurities in the system, such as the susceptor or the PAN-based carbon fiber.

Oxygen-containing impurities are believed to promote crystallization of turbostratic boron nitride.[27,28] Boron oxynitride was suggested to be an especially effective

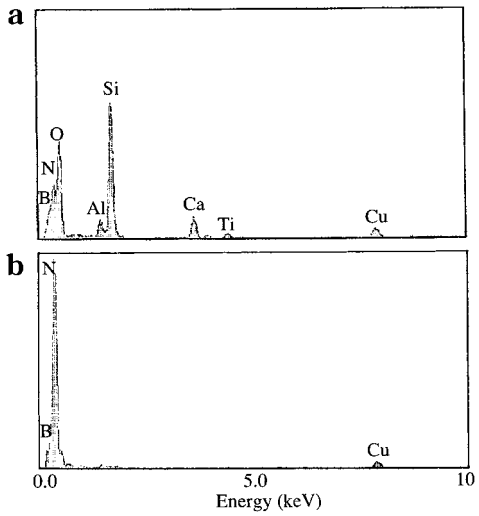

Figure 3. EDX spectra taken from the tip encapsulates and tube body, respectively. (a) Besides B−N−O, Si, Al, and Ca are detected in the tip encapsulates. (b) Only BN is detected in the tube body.

compound.[28] In the current process, it is regarded as reasonable to presume that the B−N−O nanoclusters were generated from the precursor $B_4N_3O_2H$. Simultaneously, some Si, Al, and Ca nanoclusters were also generated from impurities. Boron oxynitride (B−N−O) is not an individual, stable compound, whereas silicon- and aluminum-based oxynitridic systems are well-known as high-temperature ceramic materials.[29,30] So the B−N−O clusters may trap some modifier cations such as Si, Al, and Ca impurities during their vapor transfer to form more stable ceramic-like nanoparticles at high-temperature annealing. This kind of incorporation may be helpful to stabilize the B−N−O clusters. Once such a nanoparticle is formed and deposited on the crucible wall, BN nanotubes will form on the particle surface through precipitation and diffusion.[25,32,33] The nanotubes continually grow, with the nanoparticle moving at the head and growth directions nearly normal to the substrate, labeled the "tip-growth" model.[32,33] The tube growth terminates when the temperature decreases or the nanoparticles are fully encapsulated in the tip end.

When high-purity carbon black is used, the bulbous tips are probably formed as a way to minimize the surface energy of the B−N−O nanoclusters, as it is well-known that the minimum surface energy can be achieved in spherical clusters. On the other hand, as PAN-based carbon fiber could offer more Si and Ca impurity cations, the incorporation of these cations may stabilize the B−N−O nanoclusters into ceramic-like nanoparticles, leading to pear-shaped tip inclusions, as frequently observed for metal catalysts.[4−7,9] Though we did not carry out a systematic investigation of the optimal level of the impurities, it is worth noting that more Si

(27) Hubácek, M.; Sato, T.; Ishii, T. *J. Solid State Chem.* **1994**, *109*, 384.

(28) Kutolin, S. A.; Gashtold, V. N.; Belova, L. F. *Metody polutsheniya, svoistva i primenenie nitridov*; IPM AN USSR: Kiev, 1972.
(29) Cao, G. Z.; Metselaar, R. *Chem. Mater.* **1991**, *3*, 242.
(30) Hwang, S. L.; Chen, I. W. *J. Am. Ceram. Soc.* **1994**, *77*, 1719.
(31) Baker, R. T. K. *Carbon* **1989**, *27*, 315.
(32) Sinnott, S. B.; Andrews, R.; Qian, D.; Rao, A. M.; Mao, Z.; Dickey, E. C.; Derbyshire, F. *Chem. Phys. Lett.* **1999**, *315*, 25.
(33) Zhou, G. W.; Zhang, Z.; Bai, Z. G.; Yu, D. P. *Solid State Comm.* **1999**, *109*, 555.

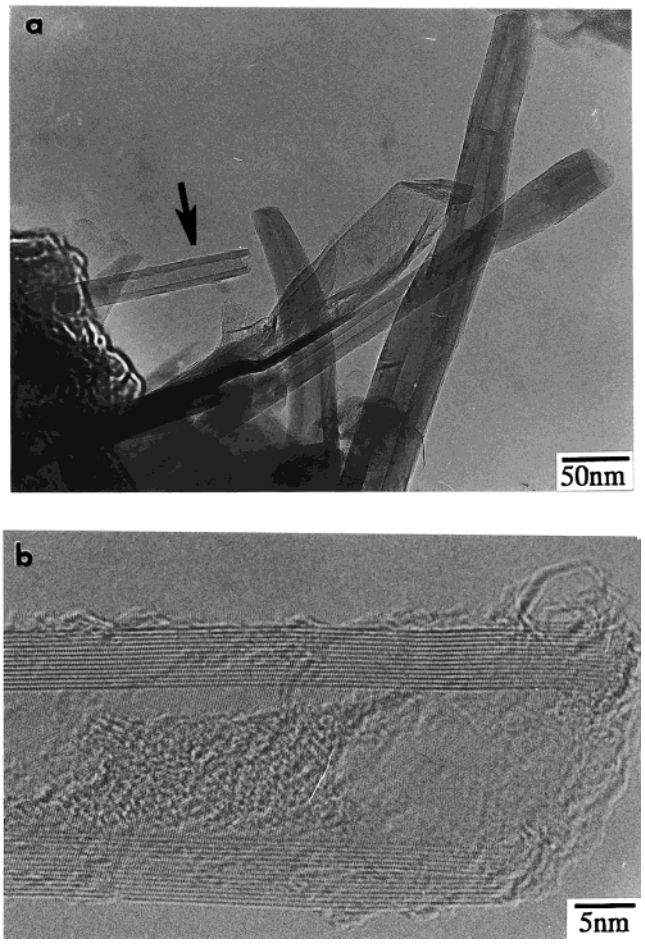

Figure 4. BN nanotubes showing open and flat tip ends. (a) Low-magnification TEM image. (b) HRTEM image of the arrowed tube in part a exhibiting open end.

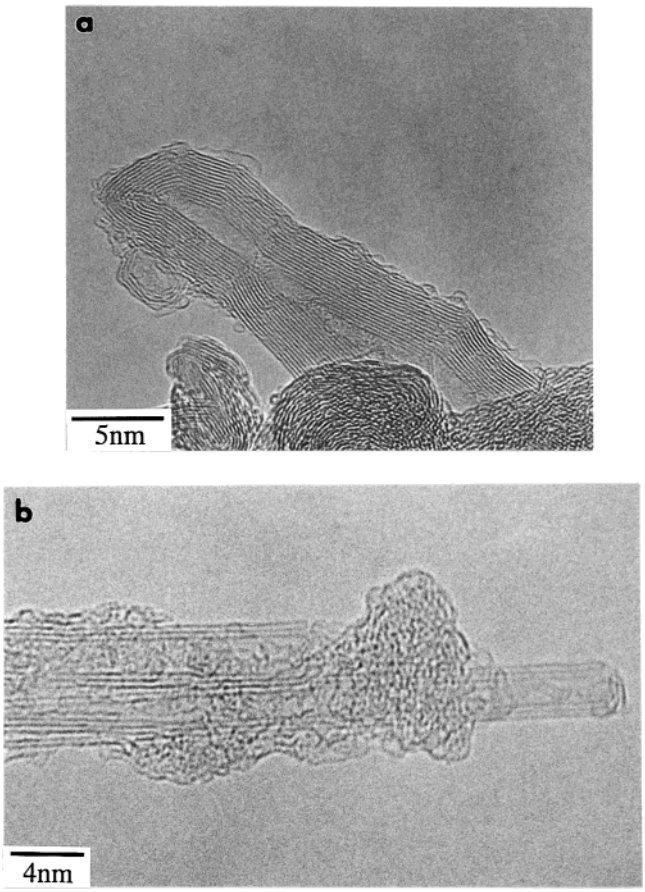

Figure 5. The closure of BN nanotubes: (a) a nanotubes changes the growth direction repeatedly before the closure, and (b) a bundle consists of two three-layer BN nanotubes; one is open while the other has a flat cap.

impurity (>1 wt %) will lead to significant Si whiskers or nanowires in the final products. Some impurities (mainly Si) may be helpful to stabilize the B−N−O nanoclusters and promote the CVD formation of BN nanotubes. But they should be controlled at a very low level.

In the samples, BN nanotubes with open or flat tip ends are occasionally observed. Figure 4a shows a low-magnification TEM image of some nanotubes with such tip characteristics. The HRTEM image of the particular nanotube (arrow) is shown in Figure 4b. The open tip end is clearly seen.

We propose that the nanotubes with open and flat tip ends are possibly formed in the open-end nanotube growth scenarios,[33] without involvement of catalyst phases. Unlike the case for carbon nanotubes, where the complete sealing is easy to achieve by introducing pentagons and heptagons, the odd-numbered topological rings are structurally unstable for BN nanotubes. This has led to the consequence that there is only a few possible specific topologies, i.e., flat or conical caps, that allow the closure of BN nanotubes. Therefore, it appears that the perfect closure of BN nanotubes is not generally feasible in CVD processes, leaving some nanotubes with open ends. In Figure 5a, a nanotube changes its growth direction repeatedly when it tends to close, until finally a nearly flat tip is achieved. A bundle consisting of two three-layer BN nanotubes is shown in Figure 5b. Even in these two neighboring nanotubes, one exhibits a flat cap while the other is open.

Open tip ends are also often observed for ceramic nanotubes (e.g., VO_x and TiO_2)[34,35] or WS_2 nanotubes,[36] in which self-sealing also appears to be possible only for certain particular, energetically preferable, topologies. Concerning the formation of open BN nanotubes from carbon nanotube templates, Golberg et al. have suggested a "scootering" effect caused by the metal atoms absorbed at the growing BN edge.[9] Such a mechanism is not considered here as there is no apparent metal catalyst used in the present method, though we cannot exclude the possibility of some metal atoms derived from the impurities in the system.

The results of a HRTEM examination of a CVD-grown multiwalled BN nanotube are shown in Figure 6a. The dark contrast lattice fringes are the tubular BN shells. They are separated by an interlayer spacing of about 0.34 nm. This is in good correspondence to the interplanar distance of 0.333 nm in bulk hexagonal (h-) BN (AA′AA′...) or rhombohedral (r-) BN (ABCABC...).[37,38]

(34) Krumeich, F.; Muhr, H. J.; Niederberger, M.; Bieri, F.; Schnyder, B.; Nesper, R. *J. Am. Chem. Soc.* **1999**, *121*, 8324.
(35) Kasuga, T.; Hiramatsu, M.; Hoson, A.; Sekino, T.; Niihara, K. *Adv. Mater.* **1999**, *11*, 1307.
(36) Zhu, Y. Q., Hsu, W. K.; Terrones, H.; Grobert, N.; Chang, B. H.; Terrones, M.; Wei, B. Q.; Kroto, H. W.; Walton, D. R. M.; Boothroyd, C. B.; Kinloch, I.; Chen, G. Z.; Windle, A. H.; Fray, D. J. *J. Mater. Chem.* **2000**, *10*, 2570.
(37) Hérold, A.; Marzluf, B.; Pério, P. *Combt. Rend.* **1958**, *246*, 1886.
(38) Paine, R. T.; Narula, C. K. *Chem. Rev.* **1990**, *90*, 73.

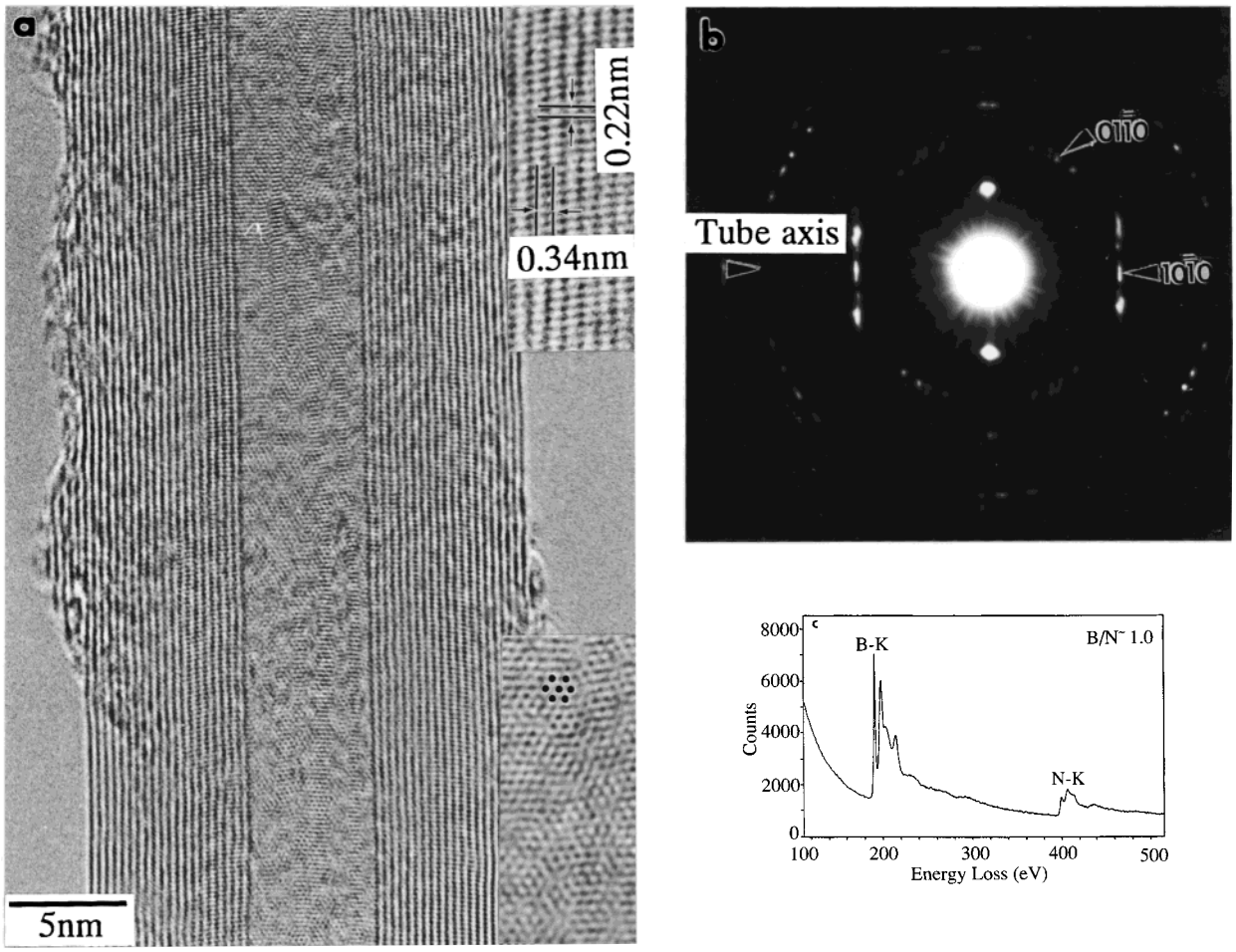

Figure 6. The structural features of the BN nanotubes and the EELS spectrum. (a) A multiwalled nanotube with uniform layer separation of 0.34 nm. (Inset on top right) The atomic columns in the wall fragments exhibiting lattice fringes separated by a average distance ~0.22 nm and the angle of 12.5° with respect to the tube axis, exhibiting r-BN stacking order. (Inset on low right) The hexagonal fringes of $10\bar{1}0$ spacing in the core region. (b) The diffraction pattern confirms the near zigzag arrangement with the $[10\bar{1}0]$ direction nearly parallel to the tube axis. (c) EELS spectrum taken from the nanotube, identifying the tube composition of boron and nitrogen with the distinct K-edge peaks at 188 and 401 eV.

Lattice fringes separated by a average distance ~0.22 nm, corresponding to the $(10\bar{1}0)$ spacing, are well-resolved in some wall fragments (inset on top right). Most of the atomic columns in the wall fragments, having an angle of 12.5° with respect to the tube axis, clearly exhibit the r-BN stacking order. The diffraction pattern (Figure 6b) reveals a near zigzag arrangement, where the $[10\bar{1}0]$ direction is nearly parallel to the tube axis. This feature is also apparent due to the hexagonal fringes of the d_{1010} spacing in the core region (inset on low right). A representative EELS spectrum taken from the tube is shown in Figure 6c. The calculated B/N ratios from numerous spectra are about 0.92 ± 0.13 (the estimated error was caused by the uncertainties in background subtraction). Therefore, the nanotube was determined to be composed of the stoichiometric BN composition.

After examining a considerable number of diffraction patterns (ca. 35), we found that most nanotubes (about 70%) synthesized by the current method exhibit the near zigzag arrangement. The preferential zigzag arrangement is consistent with the results for BN nanotubes prepared by other routes.[9,21−23] These findings suggest that zigzag BN nanotubes are probably more stable when made in experiments. Menon et al. theoretically predicted that the zigzag arrangement is energetically preferable for BN nanotubes with flat caps.[39] We also note that Blase et al. revealed that B doping leads to the preferred zigzag chirality in carbon nanotubes, where B atoms act as a surfactant during growth.[40] This model may also be applied to the zigzag geometry of BN nanotubes. The dominant zigzag arrangement in BN nanotubes constitutes an important feature. One latest report proposed that a hypothetical smart composite material reinforced by zigzag nanotubes will have useful applications in a wide variety of industries.[41]

We also observed that the r-BN stacking order dominates in our samples if only the tube wall shows clear atomic resolution. It has been concluded that cyanides play a promoting role for the formation of r-BN.[37,42] In the current process, the following chemical reaction may take place: $C + N_2 + H_2O \rightarrow 2HCN +$

(39) Menon, M.; Srivastava, D. *Chem. Phys. Lett.* **1999**, *307*, 407.
(40) Blase, X.; Charlier, J. C.; Vita, A. De.; Car, R.; Redlich, Ph.; Terrones, M.; Hsu, W. K.; Terrones, H.; Carroll, D. L.; Ajayan, P. M. *Phys. Rev. Lett.* **1999**, *83*, 5078.
(41) Srivastava, D.; Menon, M.; Cho, K. *Phys. Rev. B*, **2001**, *63*, 195413.
(42) Sato, T. *Proc. Japan Acad. Ser. B* **1985**, *61*, 459.

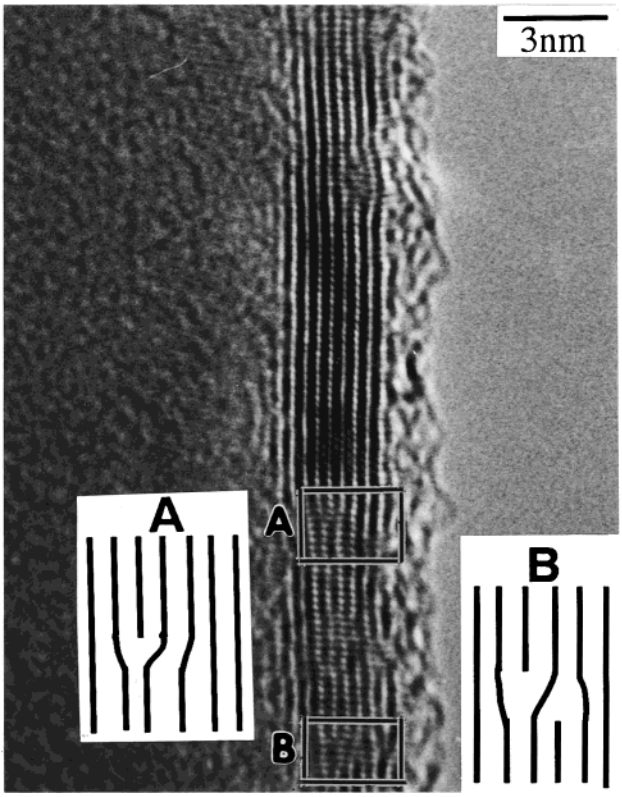

Figure 7. Layer defects and dislocations observed in the wall fragments.

CO. The so-produced cyanides are believed to play an essential role for the formation of r-BN. It may explain the reason behind the predominance of r-BN stacking.

Regardless of the tube diameter, the difference in circumference of each two consecutive cylindrical layers is $2\pi \times 0.333 \approx 2$ nm or some nine hexagonal rings of BN. Therefore, the strain is due to the addition of tube layers, and thus, three-dimension ordering in the wall fragments can only be observed in local areas. In contrast to the local three-dimension ordering, layer defects have been observed. Figure 7 shows a HRTEM image of the wall fragment of a BN nanotube. The edge dislocations in the marked area (A and B) and the severe wiggling of tube layers in the neighboring region are apparent. It seems that some layers terminate growth, possibly due to the difficulty in satisfying the stacking order and orientation relationship with respect to the previous layers, whereas the deformation of other neighboring layers occurs to stabilize the cylinder structure. Some authors concluded that kinetics rather than thermodynamics dominate the growth of BN nanotubes, because there is not sufficient time for annealing-out such growth defects.[43] Another possible reason is that the inherent strain in concentric nanotubes may be relaxed by the formation of edge dislocations.[44]

By putting some carbon fibers in the 1200 °C temperature region, BN nanotubes were also deposited on the carbon-fiber surface. Carbon fibers were selected as

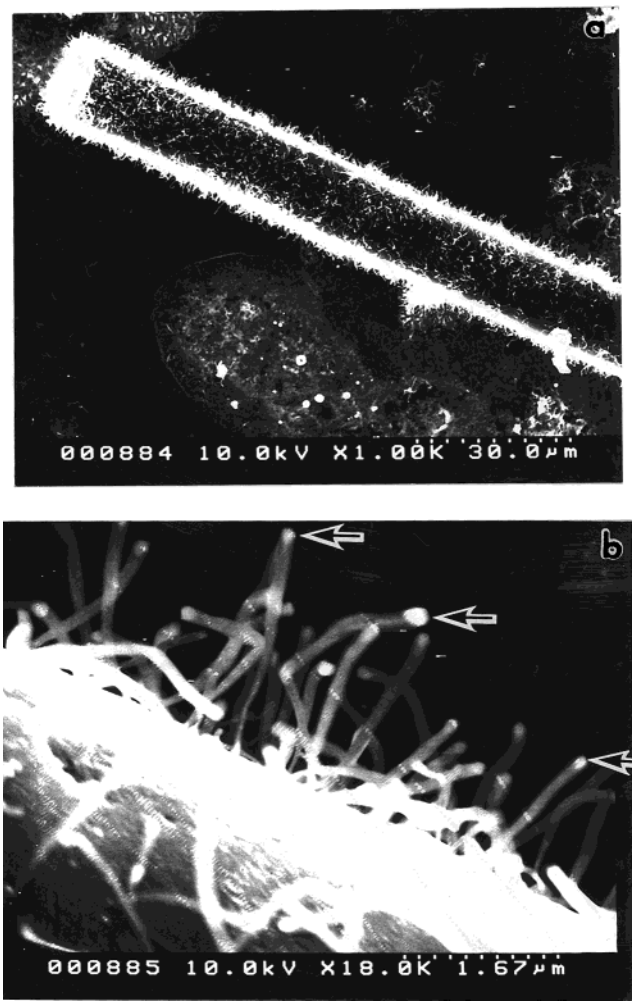

Figure 8. The results of growing BN nanotubes on carbon-fiber substrate, demonstrating the feature of being self-assembled. (a) Abundant BN tubes on the peripheral carbon surface. (b) BN nanotubes adhere to the carbon-fiber surface. Brighter encapsulates in the tips away from the substrate are apparent.

the substrate in the current work, because they may provide a deposition surface similar to the graphite crucible walls, which gave the advantages that there is no major alteration of the current growth atmosphere in the susceptor. The SEM images in Figure 8 show the SEM results of BN nanotubes grown on PAN-based carbon-fiber surface. Figure 8a exhibits abundant BN tubes on the peripheral surface. From Figure 8b, the brighter boron oxynitride inclusions, indicated by arrows, were observed in the tube ends away from the fiber surface. This strongly confirms that the particles detach and move to the head of the growing nanotubes, namely a tip-growth mechanism. The roots of the tubes remain attached to the carbon-fiber surface.

It is worth noting that the tubes grow almost vertically from the surface and show the feature of being nearly aligned. As there was no pretreatment of the carbon-fiber surface, this looks like a self-assembled growth pattern due to a possible overcrowding effect.[17] This feature should be very useful for fabricating arrays of aligned BN nanotubes, which is so far an undeveloped field in contrast to the intensive studies on controlled growth of C nanotubes.[16−19]

(43) Golberg, D.; Bando, Y.; Eremets, M.; Takemura, K.; Kurashima, K.; Tamiya, K. *Chem. Phys. Lett.* **1997**, *279*, 191.
(44) Remskar, M.; Skraba, Z.; Ballif, C.; Sanjines, R.; Levy, F. *Surf. Sci.* **1999**, *433−435*, 637.

Conclusions

Boron oxynitride nanoclusters, often stabilized by the incorporation of silicon, aluminum, and calcium, were observed as tip inclusions in the CVD growth of multiwalled BN nanotubes from a $B_4N_3O_2H$ precursor. It was suggested that these nanoclusters act as effective promoters for the formation of BN nanotubes. In addition, some nanotubes appear to be occasionally formed by the open-end growth mechanism. After examining the atomic resolution in wall fragments, the predominance of a near zigzag arrangement and rhombohedral (r-BN) stacking order in the CVD-grown BN nanotubes is revealed. BN nanotubes are observed showing self-assembled growth features on a carbon-fiber surface. This may be employed to grow large arrays of aligned BN nanotubes on other substrates for potential applications.

Acknowledgment. This work was supported by the Science and Technology Agency (STA) Fellowship at the National Institute for Materials Science (NIMS), Tsukuba, Japan.

CM0102741